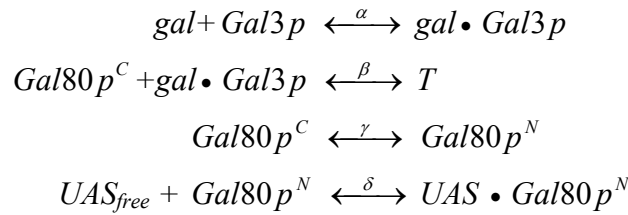


## Enhancement of cellular memory by reducing stochastic transitions *Supplementary Information*

**Modeling the galactose signalling pathway.** The regulation of gene expression in the galactose signalling pathway was modeled by separating the fast reactions such as protein-protein and protein-galactose interactions from the relatively slow mRNA synthesis. Gal3p is a cytoplasmic protein<sup>1</sup>, which gets activated upon galactose binding<sup>2,3</sup>. The activated form of Gal3p will be denoted by gal•Gal3p. Gal80p shuttles between the nucleus and the cytoplasm<sup>4</sup>. Cytosolic Gal80p (Gal80p<sup>C</sup>) binds to activated Gal3p (gal•Gal3p) whereas nuclear Gal80p, denoted by Gal80p<sup>N</sup>, binds to and inhibits the transcriptional activator, Gal4p<sup>1</sup>. Gal4p is constitutively bound to the upstream activation sequences (UAS) of most of the GAL network genes<sup>5</sup>.  $UAS_{free}$  indicates the UAS concentration not bound to Gal80p,  $UAS \bullet Gal80p$  denotes the DNA bound form of Gal80p. Gal80p is expected to exist as dimers since Gal80p dimerizes with high affinity<sup>6</sup>. The tri-molecular complex composed of Gal80p, Gal3p, and galactose is denoted by T. The fast reactions, assumed to be in equilibrium with respect to the relatively slow transcriptional processes, are:



The corresponding equilibrium constants are defined by:

$$\begin{aligned}
 \alpha &= \frac{[gal][Gal3p]}{[gal \bullet Gal3p]} \\
 \beta &= \frac{[gal \bullet Gal3p][Gal80p^C]}{[T]} \\
 \gamma &= \frac{[Gal80p^C]}{[Gal80p^N]} \\
 \delta &= \frac{[UAS_{free}][Gal80p^N]}{[UAS \bullet Gal80p^N]}
 \end{aligned} \tag{1}$$

The total concentrations of the Gal3p, Gal80p, and UAS are given by the following mass-balance equations:

$$\begin{aligned}
[Gal80p]_{Total} &= [Gal80p^C] + [Gal80p^N] + [UAS \cdot Gal80p^N] + [T] \\
[Gal3p]_{Total} &= [Gal3p] + [gal \cdot Gal3p] + [T] \\
[UAS]_{Total} &= [UAS_{free}] + [UAS \cdot Gal80p^N]
\end{aligned}
\tag{2}$$

Equations [1] and [2] are now used to determine  $[UAS_{free}]$  for a given total concentration of Gal80p, Gal3p, UAS, and galactose. This involves solving the following equation:

$$Ax + \frac{Bx}{C+x} + \frac{Dx}{E+x} - F = 0
\tag{3}$$

where,

$$\begin{aligned}
x &\equiv [Gal80p^C] \\
A &\equiv \frac{\gamma+1}{\gamma} \\
B &\equiv [Gal3p]_{Total} \\
C &\equiv \beta \left( 1 + \frac{\alpha}{[Gal]} \right) \\
D &\equiv [UAS]_{Total} \\
E &\equiv \delta\gamma \\
F &\equiv [Gal80p]_{Total} / F_0
\end{aligned}$$

In the experiments the total concentration of Gal80p is tuned by using a doxycycline inducible TET promoter. The relative concentration of Gal80p with respect to wild-type Gal80p levels (induced with 0.5 % galactose) is determined by fluorescence microscopy using strains (MA0283 and MA0291) in which Gal80p is fused to CFP. Since these measurements provide only a relative measure, the parameter  $F_0$  was introduced as a scaling factor. Equation [3] was solved using Matlab 6.0 (Mathworks, Inc.). Below we calculate the stability diagram for the Gal80p negative loop knock-out. The differential equation describing the dynamics of the core positive feedback by Gal3p is:

$$\frac{\partial [Gal3p]_{Total}}{\partial t} = k[UAS_{free}] - \Gamma[Gal3p]_{Total}
\tag{4}$$

where  $k$  and  $\Gamma$  are the rate constants for creation and destruction of Gal3p, respectively.  $[UAS_{free}]$  is determined by the solution of equation [3],  $\tilde{x}$ :

$$[UAS_{free}] = \frac{[UAS]_{total}}{1 + \tilde{x}/E} \quad [5]$$

The final goal is to determine the number of solutions of [4] in the steady-state. Defining  $\varepsilon \equiv DEk/\Gamma$  and  $z \equiv [Gal3p]_{total}/\varepsilon$  and utilizing [3], the following polynomial in  $z$  holds:

$$D_3 z^3 + D_2 z^2 + D_1 z + D_0 = 0 \quad [6]$$

where

$$\begin{aligned} D_3 &= DE^2 - \varepsilon E - CDE \\ D_2 &= AE^2 - ACE - 2DE + EF + \varepsilon + CD - CF \\ D_1 &= -2AE + AC + D - F \\ D_0 &= A \end{aligned} \quad [7]$$

If this equation has one real root the system is monostable, if it has 3 real roots it is bistable. The boundaries between the monostable and bistable regime are found by realizing that at the boundary equation [6] has exactly two real solutions and therefore equation [6] can be written as:

$$z^3 + \frac{D_2}{D_3} z^2 + \frac{D_1}{D_3} z + \frac{D_0}{D_3} = (z - a)^2 (z - b) = 0 \quad [8]$$

This results in the following conditions:

$$\begin{aligned} \frac{D_2}{D_3} &= -(2a + b) \\ \frac{D_1}{D_3} &= a^2 + 2ab \\ \frac{D_0}{D_3} &= -a^2 b \end{aligned} \quad [9]$$

Using the first two conditions results in two solutions for  $a$ :

$$\begin{aligned}
a^+ &= \frac{1}{3} \frac{D_2}{D_3} \left[ \sqrt{1 - \frac{3D_3 D_1}{D_2^2}} - 1 \right] \\
a^- &= -\frac{1}{3} \frac{D_2}{D_3} \left[ \sqrt{1 - \frac{3D_3 D_1}{D_2^2}} + 1 \right]
\end{aligned}
\tag{10}$$

In principle equations [9] and [10] can now be solved implicitly and the boundaries are obtained. However an accurate explicit form of the boundaries is found by approximating equations [10] with a second order Taylor expansion with respect to  $\frac{3D_3 D_1}{D_2^2}$ . The

advantage of the explicit method is that the experimental boundaries can be fitted directly without numerically solving [9] and [10]. Figure S7 demonstrates the accuracy of the approximate method. Substituting  $a^+$  into the last condition of [9] gives the condition for one of the phase boundaries:

$$-64D_1^2 D_2^8 - 32D_1^3 D_2^6 D_3 + 108D_1^4 D_2^4 D_3^2 + 108D_1^5 D_3^3 D_2^2 + 27D_1^6 D_3^4 + 256D_0 D_2^9 = 0$$

Since terms with high orders of  $D_2$  dominate, an adequate approximation is:

$$D_1^2 = 4D_0 D_2 \tag{11}$$

Similarly, by substituting  $a^-$  into the last condition of [9] the other boundary is found. The condition for the second boundary is:

$$2D_2^2 = 9D_3 D_1 \tag{12}$$

Relations [11] and [12] were fitted to the experimental data using  $\alpha$ ,  $F_o$ , and  $k/\Gamma$  as fit parameters. The equilibrium constants  $\beta = 0.06$  nM and  $\delta = 0.05$  nM were obtained from literature<sup>6,7</sup>. The shuttling constant  $\gamma \approx 1$  was estimated from localization studies of GFP-Gal80p<sup>1,4</sup>. The total concentration of UAS was assumed to be 50 nM based on the total number of GAL4 binding sites in the yeast genome<sup>8</sup> and an approximate nuclear volume of  $1 \mu\text{m}^3$ . The experimentally obtained boundaries (red circles, Fig. 3b) were best fitted using the parameters  $\alpha = 1\%$ ,  $F_o = 520 \mu\text{M}$ , and  $k/\Gamma = 470$ . The theoretical boundaries are denoted by the solid black lines in Fig. 3b. These parameters were subsequently used to calculate the energy landscapes and energy barriers as defined in Fig. 3c:

$$U \equiv - \int_0^{[Gal3p]_r} (k[UAS_{free}] - \Gamma[Gal3p]_{Total}) d[Gal3p]_{Total} \tag{13}$$

Note that  $[UAS_{free}]$  is a function of  $[Gal3p]_{Total}$ . Therefore, this integral has to be evaluated numerically.

**Determining experimental escape rates.** The dynamics of noise induced transitions between the two stable states of a bistable system can be studied by a three parameter model composed of the fraction of the cells in the OFF or ON states and the rates specifying the likelihood of the transitions between those two states. In what follows, the fraction of OFF-cells is represented by  $a_0$ , and that of ON-cells by  $a_1 = 1 - a_0$ . The forward and backward switching rates are denoted by  $\alpha_+$  and  $\alpha_-$ , respectively. The growth rates associated with the OFF and ON cells are assumed to be equal which is consistent with the experimentally obtained growth rates. In this analysis the stability of the fluorescent reporter YFP is ignored. Fluorescent reporters are typically very stable. However cells grow at a rapid rate and therefore dilute out the intracellular YFP at a rate that equals the cell growth rate. Since the exponential dilution rate due to cell growth ( $0.5 \text{ hour}^{-1}$ ) is much faster than the typical stochastic switching rates ( $\ll 0.1 \text{ hour}^{-1}$ , Fig. 4c), the switching rates are adequately approximated. The switching dynamics between the two states is described by the following differential equations:

$$\begin{aligned}\frac{da_0}{dt} &= \alpha_- a_1 - \alpha_+ a_0 \\ \frac{da_1}{dt} &= \alpha_+ a_0 - \alpha_- a_1\end{aligned}\tag{14}$$

Since  $a_0 + a_1 = 1$ , the solution to [14] is:

$$a_1(t) = a_1(0) + \left( \frac{\alpha_+}{\alpha_+ + \alpha_-} - a_1(0) \right) \left( 1 - e^{-(\alpha_+ + \alpha_-)t} \right)\tag{15}$$

where  $a_1(0)$  is the initial fraction of ON cells. Cells pre-grown with and without galactose will have different initial fractions defined by  $a_1(0)_G$  and  $a_1(0)_R$ , respectively.

Subtracting  $a_1(t)_R$  from  $a_1(t)_G$  leads to:

$$\alpha_+ + \alpha_- = \frac{\ln \left( \frac{a_1(0)_G - a_1(0)_R}{a_1(t)_G - a_1(t)_R} \right)}{t}\tag{16}$$

Substituting [16] in  $a_1(t)_R$ ,  $\frac{\alpha_+}{\alpha_+ + \alpha_-}$  is found:

$$\frac{\alpha_+}{\alpha_+ + \alpha_-} = \frac{a_1(t)_R - a_1(0)_R + a_1(0)_R \left( 1 - \frac{a_1(t)_G - a_1(t)_R}{a_1(0)_G - a_1(0)_R} \right)}{1 - \frac{a_1(t)_G - a_1(t)_R}{a_1(0)_G - a_1(0)_R}} \quad [17]$$

Since the initial fractions ( $a_1(0)_R, a_1(0)_G$ ) and fractions at a specific time ( $a_1(t)_R, a_1(t)_G$ ) are experimentally known, the escape rates  $\alpha_+$  and  $\alpha_-$  for the two stable states can be estimated.

**Doxycycline inducible  $P_{TET}$  system** To externally control the Gal3p and Gal80p levels in strains MA0182 and MA0188 respectively, the *GAL3* and *GAL80* genes were placed under the control of the  $P_{TET}$  promoter. In the presence of doxycycline, this promoter is activated by the transcriptional activator rtTA, comprised of the VP16 activator and the TetR(S2) DNA binding domains. rtTA was chosen to control the Gal3p and Gal80p levels, since it is a transcriptional activator with a broad regulatory range<sup>9</sup>.

### Supplementary references:

1. Peng, G. & Hopper, J.E. Gene activation by interaction of an inhibitor with a cytoplasmic signaling protein. *Proc. Natl. Acad. Sci. USA* **99**, 8548-8553 (2002).
2. Timson, D. J., Ross, H. C. & Reece, R. J. Gal3p and Gal1p interact with the transcriptional repressor Gal80p to form a complex of 1:1 stoichiometry. *Biochem. J.* **363**, 515–520 (2002).
3. Suzuki-Fujimoto, T., Fukuma, M., Yano, K. I., Sakurai, H., Vonika, A., Johnston, S. A. & Fukasawa, T. Analysis of the galactose signal transduction pathway in *Saccharomyces cerevisiae*: interaction between Gal3p and Gal80p. *Mol. Cell. Biol.* **16**, 2504-2508 (1996).
4. Peng, G. & Hopper, J. E. Evidence for Gal3p's Cytoplasmic Location and Gal80p's Dual Cytoplasmic-Nuclear Location Implicates New Mechanisms for Controlling Gal4p Activity in *Saccharomyces cerevisiae*. *Mol. Cell. Biol.* **20**, 5140-5148 (2000).
5. Mizutani, A. & Tanaka, M. Regions of GAL4 critical for binding to a promoter in vivo revealed by a visual DNA-binding analysis. *EMBO J.* **22**, 2178-2187 (2003).
6. Melcher, K. & Xu, H. E. Gal80–Gal80 interaction on adjacent Gal4p binding sites is required for complete GAL gene repression. *EMBO J.* **20**, 841–851 (2001).
7. Verma, M., Bhat, P. J. & Venkatesh, K. V. Quantitative Analysis of GAL Genetic Switch of *Saccharomyces cerevisiae* Reveals That Nucleocytoplasmic Shuttling of Gal80p Results in a Highly Sensitive Response to Galactose. *J. Biol. Chem.* **278**, 48769-48769 (2003).
8. Ren, B. *et al.* Genome-wide location and function of DNA binding proteins. *Science* **290**, 2306–2309 (2000).
9. Urlinger, S. *et al.* Exploring the sequence space for tetracycline-dependent transcriptional activators: novel mutations yield expanded range and sensitivity. *Proc. Natl. Acad. Sci. U. S. A.* **97**, 7963-7968 (2000).

Supplementary Figure 1.

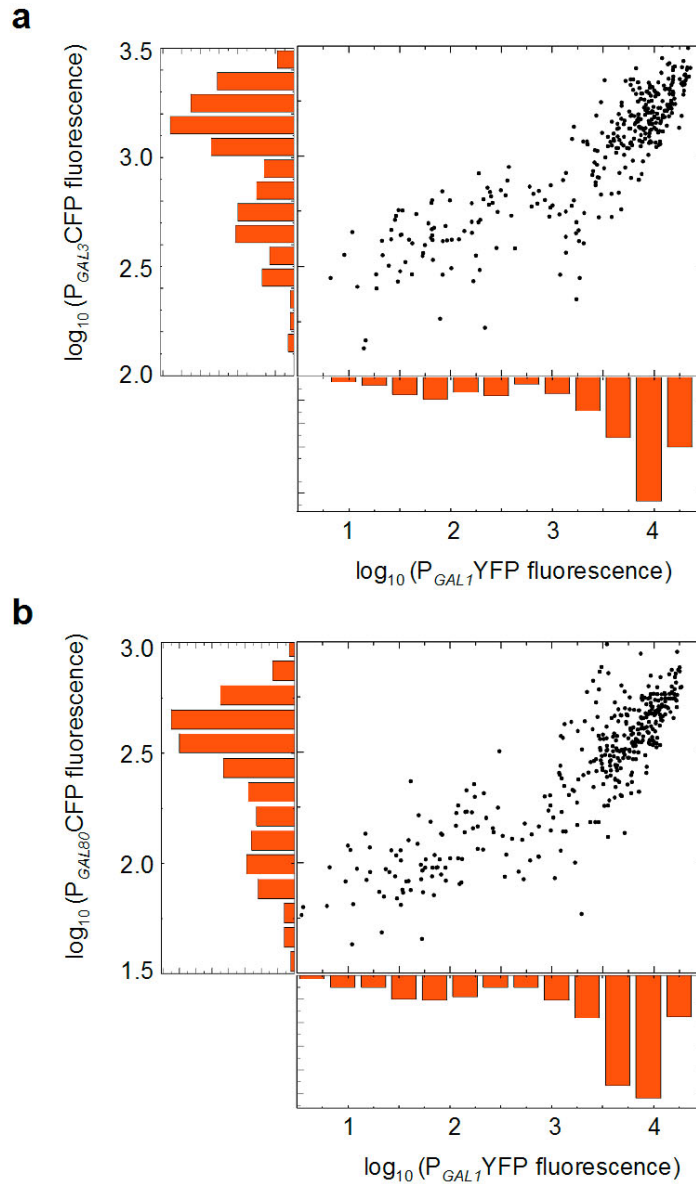


**Figure S1.** Single-cell two-color correlation experiments. **a**, Activities of *GAL1* and *GAL3* promoters driving YFP and CFP, respectively, were measured using fluorescence microscopy (strain MA0231). **b**, Activities of *GAL1* and *GAL80* promoters driving YFP and CFP, respectively, were measured using fluorescence microscopy (strain MA0242). 0.040% Galactose has been used to induce ‘raffinose history’ cells for 27 hours. Both histograms and the scatter plots indicate a strong correlation between the activities of the two promoters in single cells. We corrected for bleed-through between the CFP and YFP filters.

Supplementary Figure 2.

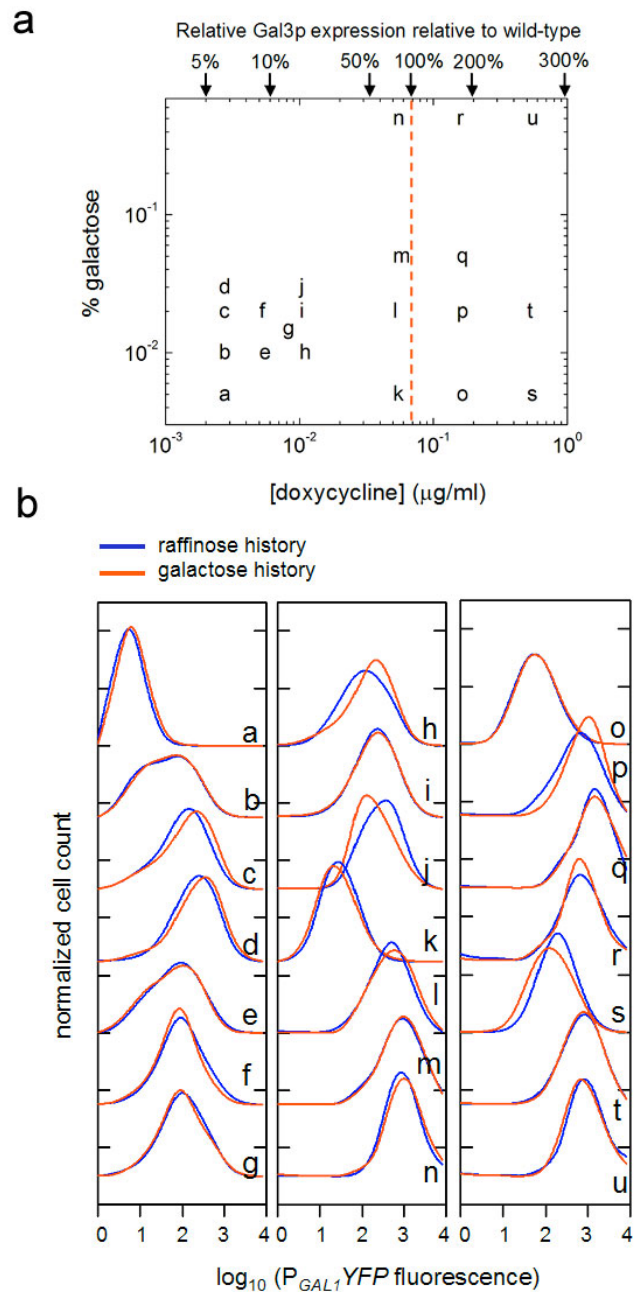


**Figure S2.** Loss of memory in the *GAL3* loop knock out (strain MA0182). **a**, Galactose and doxycycline concentrations are indicated for each experiments shown in **b**. The amount of Gal3p driven by the doxycycline inducible TET promoter is indicated relative to the wild-type expression (when induced with 0.5% galactose for 27 hours) as determined by fluorescence microscopy using Gal3p-CFP fusion proteins. The red dotted line represents the wild-type Gal3p level. **b**, MA0182 strain expression histograms (after 27 hr induction period) for a wide range of galactose and doxycycline concentrations.

### Supplementary Figure 3.

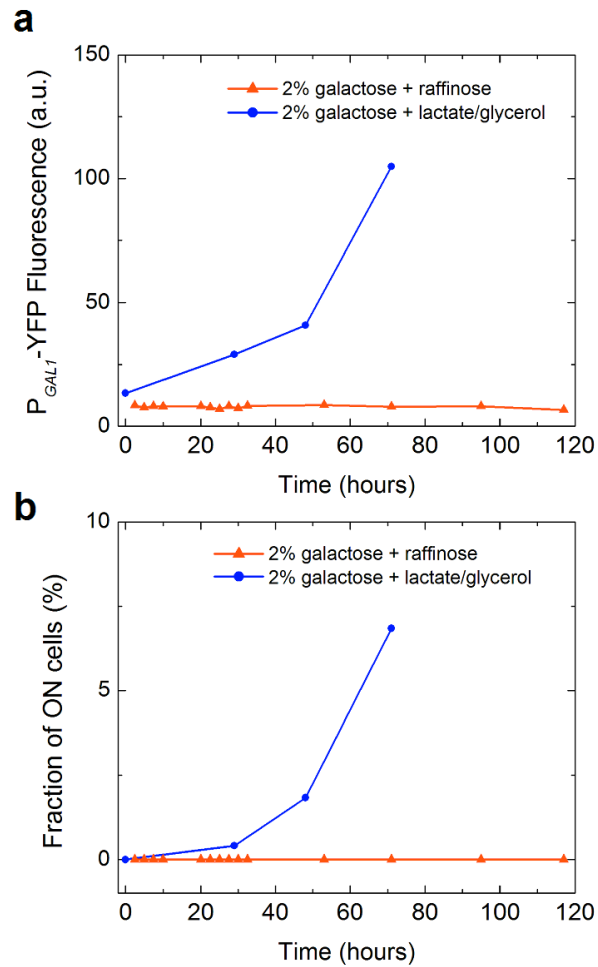


**Figure S3.** Occurrence of long-term adaptation in media with various carbon sources. **a**, Population averaged YFP levels in *gal3Δ* cells (strain MA0226) as a function of time for which the cells were induced with 2% galactose. **b**, Fraction of YFP expressing cells (strain MA0226) as a function of time. Long-term adaptation is not observed using synthetic media containing 2% raffinose and 2% galactose (red triangles). However when YEP is supplemented with 3% glycerol, 2% lactate, and 2% galactose (blue circles) long-term adaptation is observed as early as 30 hours after addition of 2% galactose to the media.

Supplementary Figure 4.

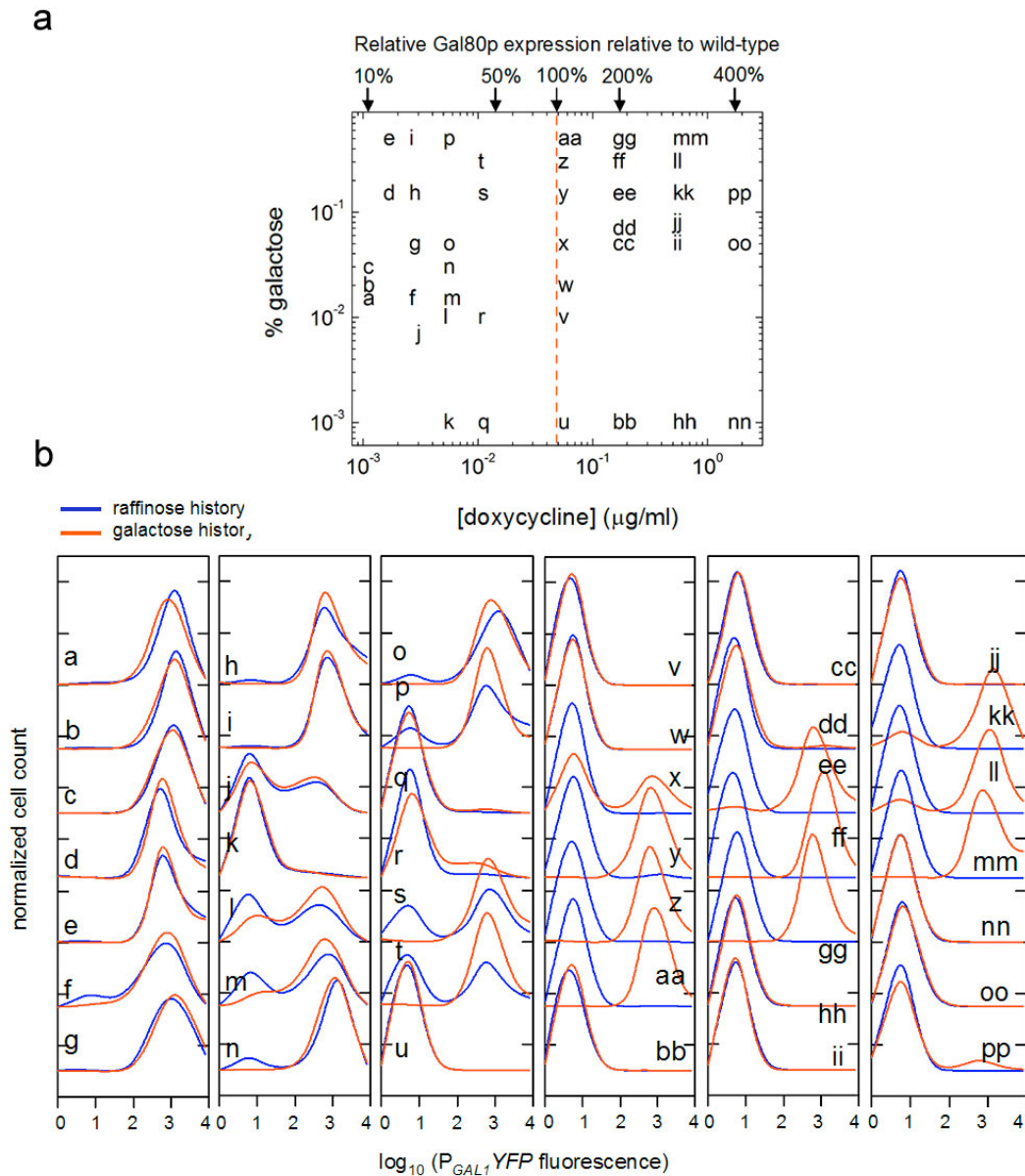


**Figure S4.** Behaviour of the *GAL80* loop knock out (strain MA0188). **a**, Galactose and doxycycline concentrations are indicated for each experiments shown in **b**. The amount of Gal80p driven by the doxycycline inducible TET promoter is indicated relative to the wild-type expression (when induced with 0.5% galactose for 27 hours) as determined by fluorescence microscopy using Gal80p-CFP fusion proteins. The red dotted line represents wild-type levels of Gal80p. **b**, MA0188 expression histograms (after 27 hr induction period).

Supplementary Figure 5.

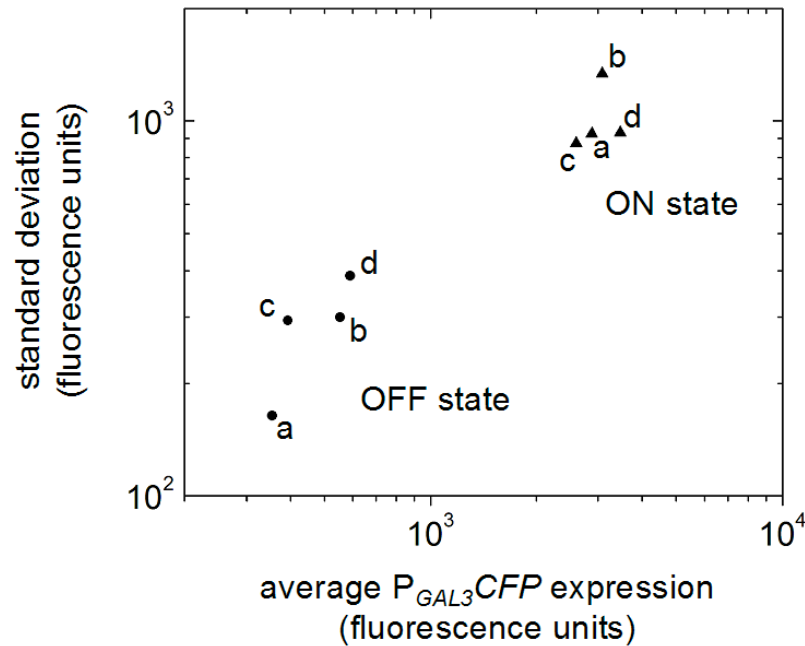


**Figure S5.** The role of Gal3p fluctuations in stochastic transitions. Raffinose history cells (strain MA0239) were induced with four different concentrations of galactose and doxycycline for 27 hours, each letter corresponding to a specific set of galactose and doxycycline: **a** 0 % galactose, 0  $\mu\text{g/ml}$  doxycycline, **b** 0.004% galactose, 0.00185  $\mu\text{g/ml}$  doxycycline, **c** 0.007% galactose, 0.0031  $\mu\text{g/ml}$  doxycycline, **d** 0.017% galactose, 0.00685  $\mu\text{g/ml}$  doxycycline. Fluorescence microscopy was used to determine CFP levels in individual cells. The resulting histograms were analyzed to determine the average  $P_{GAL3}CFP$  expression and the standard deviation (as a measure of  $GAL3$  fluctuations) for both OFF and ON state.

## Supplementary Figure 6.

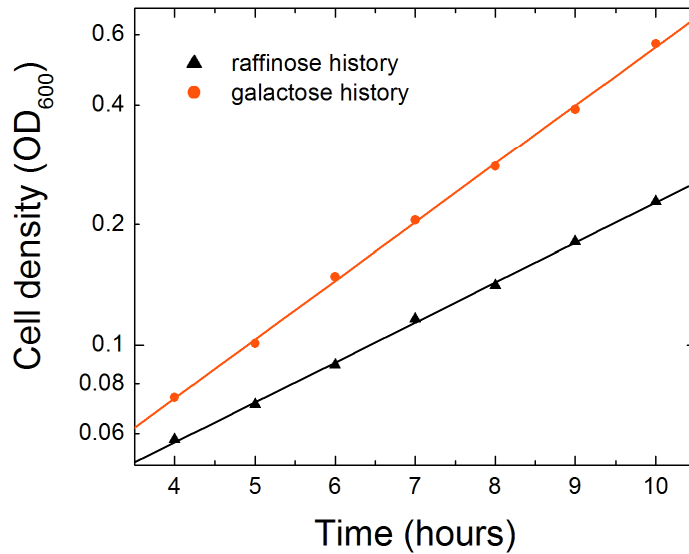


**Figure S6.** Growth rate is affected by history. Two populations of MA0188 cells (*gal80Δ P<sub>TET</sub>GAL80*) were prepared with a raffinose and galactose history in the persistent memory region (0.25% galactose, 0.15 μg/ml doxycycline, 2% raffinose) for 27 hours. Subsequently these cells were washed and transferred to media lacking raffinose but having the same concentration of galactose and doxycycline (0.25% galactose, 0.15 μg/ml doxycycline). After a lag phase of about 4 hours an exponential growth for both histories is observed, however, the galactose history cells divide at a rate that is about 1.5 fold larger than the raffinose history cells.

Supplementary Figure 7.

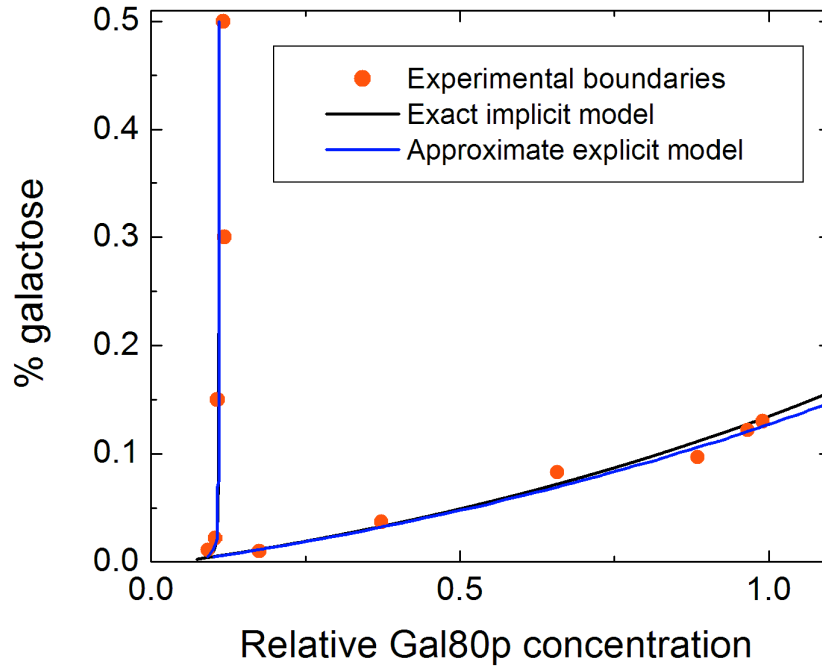


**Figure S7.** Phase boundaries determined by the approximate explicit method and the exact implicit method. For the left boundary both methods yield indistinguishable results. For large relative Gal80p concentrations the approximate result deviates slightly with respect to the exact result.

**Supplementary Table 1.** Yeast strains used in this study:

<b>Strain</b>	<b>Genotype</b>
MA0182	<i>MATa/α, ura3/ura3::URA3-P<sub>TETO2</sub>-GAL3, his3::HIS3/his3, ade2::ADE2-P<sub>MYO2-rtTA/ade2</sub>::ADE2-P<sub>GAL1</sub>-YFP, gal3Δ::KanMX/gal3Δ::KanMX</i>
MA0188	<i>MATa/α, ura3/ura3::URA3-P<sub>TETO2</sub>-GAL80, his3::HIS3/his3, ade2::ADE2-P<sub>MYO2-rtTA/ade2</sub>::ADE2-P<sub>GAL1</sub>-YFP, gal80Δ::KanMX/gal80Δ::KanMX</i>
MA0207	<i>MATa/α, his3::HIS3/his3, ade2/ade2::ADE2-P<sub>GAL1</sub>-YFP</i>
MA0208	<i>MATa/α, ura3/ura3::URA3, his3::HIS3/his3, ade2/ade2::ADE2-P<sub>GAL2</sub>-YFP</i>
MA0210	<i>MATa/α, ura3/ura3::URA3, his3::HIS3/his3, ade2/ade2::ADE2-P<sub>GAL4</sub>-YFP</i>
MA0211	<i>MATa/α, ura3/ura3::URA3, his3::HIS3/his3, ade2/ade2::ADE2-P<sub>GAL6</sub>-YFP</i>
MA0212	<i>MATa/α, ura3/ura3::URA3, his3::HIS3/his3, ade2/ade2::ADE2-P<sub>GAL7</sub>-YFP</i>
MA0213	<i>MATa/α, ura3/ura3::URA3, his3::HIS3/his3, ade2/ade2::ADE2-P<sub>GAL10</sub>-YFP</i>
MA0215	<i>MATa/α, ura3/ura3::URA3, his3::HIS3/his3, ade2::ADE2-P<sub>MYO2-rtTA/ade2</sub>::ADE2-P<sub>GAL1</sub>-YFP, gal2Δ::KanMX/gal2Δ::KanMX</i>
MA0226	<i>MATa/α, ura3/ura3::URA3, his3::HIS3/his3, ade2::ADE2-P<sub>MYO2-rtTA/ade2</sub>::ADE2-P<sub>GAL1</sub>-YFP, gal3Δ::KanMX/gal3Δ::KanMX</i>
MA0231	<i>MATa/α, ura3/ura3::URA3, his3::HIS3/his3, ade2::ADE2-P<sub>GAL3</sub>-CFP/ade2::ADE2-P<sub>GAL1</sub>-YFP</i>
MA0239	<i>MATa/α, ura3/ura3::URA3-P<sub>TETO2</sub>-GAL80, his3::HIS3/his3, ade2::ADE2-P<sub>MYO2-rtTA/ade2</sub>::ADE2-P<sub>GAL1</sub>-YFP, trp1::TRP1-P<sub>GAL3</sub>-CFP/trp1, gal80Δ::KanMX/gal80Δ::KanMX</i>
MA0242	<i>MATa/α, ura3/ura3::URA3, his3::HIS3/his3, ade2::ADE2-P<sub>GAL80</sub>-CFP/ade2::ADE2-P<sub>GAL1</sub>-YFP</i>
MA0273	<i>MATa/α, ura3/ura3::URA3-P<sub>TETO2</sub>-GAL3-CFP, his3::HIS3/his3, ade2::ADE2-P<sub>MYO2-rtTA/ade2</sub>::ADE2-P<sub>GAL1</sub>-YFP</i>
MA0282	<i>MATa/α, ura3/ura3::URA3-P<sub>GAL3</sub>-GAL3-CFP, his3::HIS3/his3, ade2::ADE2-P<sub>MYO2-rtTA/ade2</sub>::ADE2-P<sub>GAL1</sub>-YFP, gal3Δ::KanMX/GAL3</i>
MA0283	<i>MATa/α, ura3/ura3::URA3-P<sub>GAL80</sub>-GAL80-CFP, his3::HIS3/his3, ade2::ADE2-P<sub>MYO2-rtTA/ade2</sub>::ADE2-P<sub>GAL1</sub>-YFP, GAL80/gal80Δ::KanMX</i>
MA0291	<i>MATa/α, ura3/ura3::URA3-P<sub>TETO2</sub>-GAL80-CFP, his3::HIS3/his3, ade2::ADE2-P<sub>MYO2-rtTA/ade2</sub>::ADE2-P<sub>GAL1</sub>-YFP</i>

**Supplementary Table 2.** Galactose depletion experiments

Construct	Galactose consumption rate $c$ (mM·(OD <sub>600</sub> ·hours) <sup>-1</sup> )	Density of culture when galactose concentration changes by 10% (OD <sub>600</sub> ) <sup>†</sup>
WT	0.084±0.010	0.431
<i>gal80Δ</i> P <sub>TET</sub> GAL80	0.062±0.041	0.574
<i>gal3Δ</i> P <sub>TET</sub> GAL3	0.639±0.083	0.056

<sup>†</sup> The density of the culture was calculated from  $kg/c$ , where  $k$  is cell division rate,  $g$  is the change in galactose concentration.  $g=0.002\%$ , which corresponds to a 10% change when the initial galactose concentration is 0.020%. At the beginning of the experiment OD<sub>600</sub> = 10<sup>7</sup>. A concentration of 30 μg/ml doxycycline was used to obtain a maximum *GAL3* and *GAL80* expression.